Anchor-Guiding Mechanism for Beacon-Assisted Localization in Wireless Sensor Networks

Chao-Tsun Chang, Chih-Yung Chang, *Associate Member, IEEE*, and Chih-Yu Lin

***Abstract*—Localization is one of the most important issues in wireless sensor networks (WSNs). In the most widely proposed range-free algorithms, nodes estimate location by employing the geometric constraints imposed by the location of the mobile anchor. However, none of them addresses how the mobile anchor moves to optimize the improvement of location inaccuracies and minimize the anchor's movement. This paper assumes that previous range-free algorithms have been executed for a period of time and the deployed sensors are of different location inaccuracies. According to the size of the estimative region of each static sensor, an anchor-guiding mechanism is proposed to determine the beacon locations and construct an efficient path for the mobile anchor. Experimental study reveals that the proposed anchor-guiding mechanism effectively guides the mobile anchor to move along an efficient path, thereby saving the time required for improving or balancing the location inaccuracies of all sensor nodes.**

***Index Terms*—Location estimates, mobile anchor, path guiding, wireless sensor networks.**

I. Introduction

LOCATION awareness of sensor nodes plays a critical role in most sensor network applications such as coverage calculation, event detection, object tracking, and location aware routing. The sensor nodes have to be aware of their location to specify "where" a certain event takes place. Determining the physical location of the sensors after they have been deployed is known as the problem of localization.

Many mechanisms have been proposed to address the range-free localization problem [1]–[3]. These schemes [4]–[15] share the common feature of deploying beacon nodes (also called anchors) that are aware of their own location information in the WSN. All the other sensor nodes discover their locations based on the information provided by the anchors. The anchor-based localization schemes are categorized into static and mobile anchor techniques. The common challenge of static anchor schemes is that the location inaccuracy of each sensor node highly depends on the number and the deployed positions of the static anchors. To improve location inaccuracy, the number of anchor nodes tends to be increased, which adds to the localization cost. Another problem of static anchors is that they do not perform any other function after broadcasting the beacons [7].

To eliminate the need for static anchors, studies [4]–[15] propose some schemes based on a mobile anchor for a resource-constrained WSN. The mobile anchor is aware of its own location information with the use of GPS or other location support system. It moves and broadcasts its coordinates at some certain locations, which can be treated as virtual static anchors at those locations. Each static sensor that receives the mobile anchor's coordinates is aware that its location is within the communication range of the mobile anchor. Therefore, the static sensor can identify that it is located within a specific region. When a static sensor receives different coordinates from the mobile anchor, it can calculate its new estimative region by the intersection of all possible location regions based on the received coordinates. However, these studies do not consider how the mobile anchor moves and where the beacon should be broadcasted, especially when the static sensors have different location inaccuracies in the given WSN. To this end, this paper aims to develop an anchor-guiding mechanism for the mobile anchor to improve the location inaccuracies of all sensors and minimize the anchor's movement.

The remaining part of this paper is organized as follows. Section II gives related work of localization mechanisms while Section III illustrates the network environment and problem formulation of the proposed guiding mechanism. Section IV details the proposed anchor-guiding mechanisms while Section V analyzes the guiding efficiency of the proposed scheme. Section VI investigates the performance of the proposed guiding mechanism and then the conclusion is given in Section VII.

II. Related Work

Localization with low cost and high accuracy is of utmost importance for most applications in WSNs. To eliminate the hardware cost such as a GPS device on each static sensor or even remove the requirement of deploying a number of static anchors in the WSN, a number of localization schemes [8], [9] have been proposed for a resource-constrained WSN.

In studies [4]–[6], [8]–[11], a mobile anchor being aware of its own location is proposed to periodically move and broadcast a beacon with its current coordinate for improving the location inaccuracy of the nearby static sensors. Upon receiving the beacon message, the sensor node indicates that it is within

Manuscript received July 13, 2011; revised August 16, 2011; accepted August 16, 2011. Date of publication August 22, 2011; date of current version April 11, 2012. This work was supported in part by the National Science Council of the Republic of China under Contract NSC 100-2221-E-032-015-MY3 and Contract NSC 100-2632- E-032-001-MY3. The associate editor coordinating the review of this manuscript and approving it for publication was Dr. Subhas Mukhopadhyay.

C.-T. Chang is with the Department of Information Management, Hsiuping University of Science and Technology, Dali, Taichung 41280, Taiwan (e-mail: cctas@mail.hust.edu.tw).

C.-Y. Chang and C.-Y. Lin are with the Department of Computer Science and Information Engineering, Tamkang University, Tamsui, Taipei 25137, Taiwan (e-mail: cychang@mail.tku.edu.tw; cylin@wireless.cs.tku.edu.tw).

Color versions of one or more of the figures in this paper are available online at http://ieeexplore.ieee.org.

Digital Object Identifier 10.1109/JSEN.2011.2165943

the region of the circle centered at the coordinate of mobile anchor with a radius of r, where r is the communication range of the mobile anchor. Therefore, the sensor node identifies that its location is within the circle region, which is referred to the *estimative region*. Based on the range-constraint of beacon messages, a static sensor that receives several different coordinates from the mobile anchor may reduce its estimative region by calculating the intersected estimative region of its neighbors and itself, hence improving the location inaccuracy. However, the range-constraint localization is mainly applied by those sensors that are actually one-hop neighbors of the mobile anchor.

Srinath T. V. [7] extends the range-constraint from one-hop to the two-hop neighboring sensors. Let $A = \{a_1, a_2, \ldots, a_n\}$ denote the set of n neighbors of the mobile anchor and B_i denote those sensors that neighbor to sensor a_i in set A. Upon receiving the location information from the mobile anchor, all sensors in set A calculate their estimative regions and then broadcast the regions to their neighbors. Since the two-hop neighboring sensors of mobile anchor cannot receive the location information from mobile anchor, nodes in set B_i have a location constraint that they are not located in the estimative region of a_i. However, since nodes in set B_i neighbor to node a_i, they have another constraint that they are located in the communication range of any possible location of a_i. Based on these two constraints, nodes in set B_i can also derive their own estimative regions.

Utilizing different coordinates received from the mobile anchor might reduce the static sensor's estimative region, consequently improving the location inaccuracy. However, it is complex and time consuming to calculate the intersection region of several circle regions. Some other studies [8], [9] propose localization schemes applying a rectangle region instead of a circle region to simplify both the calculation and representation of the new estimative region. However, given a WSN, it is an essential requirement that the localization task should be completed under the constraint of the anchor's remaining energy. The previous studies failed to address how the mobile anchor can achieve the optimal improvement of location inaccuracy for the WSN.

This paper presents an important observation that the improvement of sensors' location inaccuracies highly depends on the beacon locations that determine the movement path of the mobile anchor. Let ER_s denote the current estimative region of sensor s. Let the communication range of the mobile anchor be r and the new beacon coordinate received by sensor s be (x, y). The new range-constraint of sensor s will be the square region R where the left-up and the right-down points are with coordinates $(x - r, y - r)$ and $(x + r, y + r)$, respectively. The new estimative region of sensor s is the intersected region of the old estimative region ER_s and the new range-constraint R. This also indicates that the improvement of the estimative region is the region area $ER_s - R$, which is contributed from the receipt of the new beacon. As a result, given the ER_s of sensor s, the improvement of the ER_s highly depends on the new beacon location (x, y). Therefore, there are two important tasks for a mobile anchor in improving the location inaccuracy of the WSN: *determining the promising beacon locations* and *constructing an efficient path* that passes through these locations with minimal path length.

III. Network Environment and Problem Statement

1) Network Environment: Let the *monitoring region* be the region where users are interested to monitor. To totally understand what events occur in the monitoring region, a large number of sensors will be deployed in the region to detect the event and report their sensing information via multi-hop routing. This paper considers that a large number of static sensors have been randomly deployed in the monitoring region. Assume that localization schemes proposed in [4]–[15] have been applied to the monitoring region for a while such that all sensors might have different initial estimative regions. During the execution of the existing localization schemes, the mobile anchor can also collect the information of estimative regions of these sensors. Herein, we notice that our work is complementary to the existing studies [4]–[15] and can be applied after each sensor has an initial estimative region.

In addition, the mobile anchor m that is always aware of its own location information by GPS or other location support system. The communication ranges, denoted by r, of the mobile anchor and all static sensors are equal. Consider that the mobile anchor m broadcasts a beacon at location (x_m, y_m) at time t. The beacon $b(x_m, y_m)_t$ that indicates the current location (x_m, y_m) of mobile anchor at time t will create a new range-constraint $R_t(x_m, y_m) = [(x_m - r, y_m - r), (x_m + r, y_m + r)]_t$.

We assume that each static sensor s has an initial rectangle estimative region $ER_{s,t} = [(x_{s,1}, y_{s,1}), (x_{s,2}, y_{s,2})]_t$ of its location at time t, where coordinates $(x_{s,1}, y_{s,1})$ and $(x_{s,2}, y_{s,2})$ denote the locations of left-up and right-down points of $ER_{s,t}$. The size of $ER_{s,t}$ can be evaluated by $|x_{s,2} - x_{s,1}| \times |y_{s,2} - y_{s,1}|$.

2) Problem Formulation: A beacon $b(x_m, y_m)_{t'}$ broadcasted by the mobile anchor m at time t' will create a new range-constraint region, called *broadcasting rectangle* $R_{t'}(x_m, y_m)$, to those static sensors neighboring to the mobile anchor. Upon receiving the beacon at time $t' > t$, the sensor s will recalculate its estimative region by

$$ER_{s,t'} = ER_{s,t} \cap R_{t'}(x_m, y_m). \quad (1)$$

Fig. 1 depicts an example of the calculation of $ER_{s,t'}$ when sensor s receives a beacon $b(x_m, y_m)_{t'}$. The dotted rectangle in Fig. 1 represents the estimative region $ER_{s,t}$ of sensor s at time t while a new range-constraint $R_{t'}(x_m, y_m)$ is represented by the solid square. The sensor s uses the received beacon information and applies Equation (1) to determine the new estimative region $ER_{s,t'}$ (depicted by the shadow region). To simplify the calculation of $ER_{s,t'}$, a solid square is used instead of the dotted circle. As shown in Fig. 1, since the area size of $ER_{s,t'}$ is smaller than that of $ER_{s,t}$, the location inaccuracy of sensor s can be improved.

In the randomly deployed WSN, the estimative regions of sensors might be different because these sensors receive several different beacons from the mobile anchor m. The locations

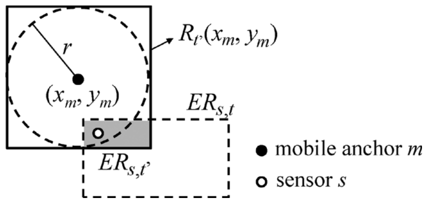

Fig. 1. An example that illustrates the calculation of new estimative region $ER_{s,t'}$ of sensor s when it receives a beacon $b(x_m, y_m)_{t'}$ from mobile anchor m.

where the mobile anchor broadcasts beacons will result in different improvements on the location inaccuracy of WSN. Let $bef_{s(x_m,y_m)}$ and $bef_{(x_m,y_m)}$ denote the benefits of sensor s and all sensors obtained from the beacon $b(x_m, y_m)_{t'}$, respectively. If a static sensor s with the estimative region $ER_{s,t}$ receives a beacon $b(x_m, y_m)_{t'}$ from mobile anchor m, the improvement of its location inaccuracy can be measured by

$$\begin{aligned} bef_{s(x_m,y_m)} &= ER_{s,t} - ER_{s,t'} \\ &= ER_{s,t} - (ER_{s,t} \cap R_{t'}(x_m, y_m)). \end{aligned} \quad (2)$$

Let $N(m)$ denote the sensors that neighbor to the mobile anchor m. Equation (3) shows the total benefits obtained from the beacon

$$bef_{(x_m,y_m)} = \sum_{s_i \in N(m)} bef_{s_i(x_m,y_m)}. \quad (3)$$

3) The Investigated Problem: This paper aims at developing a guiding mechanism that constructs a path passing through all beacon locations to obtain maximal benefits and minimize the movement of the mobile anchor. Assume that the proposed guiding mechanism constructs a path p passing through k beacon locations $l_1 = (x_1, y_1), l_2 = (x_2, y_2), \ldots,$ and $l_k = (x_k, y_k)$, where there are i turns on path p. When the anchor arrives at beacon location l_i, the mobile anchor will stop to broadcast a beacon and then move or turn toward the next beacon location along path p. Let E_m denote the total energy consumption of the mobile anchor in the anchor guiding process. The E_m can be derived by the energy consumptions required for moving along path p, for stopping and broadcasting the beacons, and for making turns. Let e_p, e_{stop}, e_{beacon} and e_{turn} denote the energy consumptions for mobile anchor moving per unit distance, stopping once, broadcasting a beacon, and making a turn, respectively. Let $|p|$ denote the length of path p. Furthermore, assume that there are i turns and k stops for broadcasting k beacons on path p. The E_m can be represented by

$$\begin{aligned} E_m &= \text{energy consumption for moving in the path} \\ &\quad + \text{energy consumption for stopping} \\ &\qquad \text{and broadcasting the beacons} \\ &\quad + \text{energy consumption for making turns} \\ &= |p| \times e_p + k \times (e_{stop} + e_{beacon}) + i \times e_{turn}. \end{aligned} \quad (4)$$

Let E_c is the initial energy of mobile anchor. The total benefit of the anchor's movement and beacons should be maximized under the constraint $E_m \leq E_c$. The total benefit $Total\_bef$ is calculated as shown in

$$Total\_bef = \sum_{1 \leq i \leq k} bef_{(x_i,y_i)}. \quad (5)$$

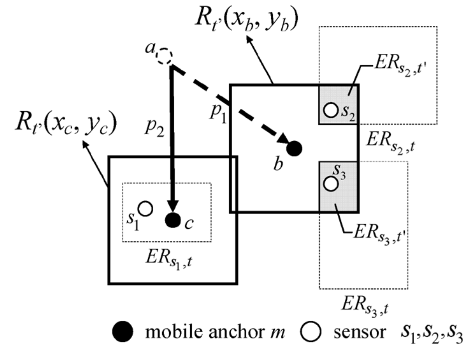

Fig. 2. Mobile anchor moving along path p_1 and broadcasting a beacon at location b will contribute more benefits for localization than moving along path p_2 and broadcasting a beacon at location c.

Fig. 2 shows an example of a mobile anchor moving along different paths and broadcasting beacons at different locations resulting in different contributions for improving the location inaccuracy of the WSN. At time t, the three static sensors s_1, s_2 and s_3 have estimative regions: $ER_{s_1,t}$, $ER_{s_2,t}$ and $ER_{s_3,t}$, respectively, which are represented by the dotted rectangles in Fig. 2. Assume that the current location of mobile anchor is a. In case that mobile anchor moves along path p_2 and broadcasts a beacon at location $c = (x_c, y_c)$, the new range-constraint $R_{t'}(x_c, y_c)$ does not help for improving the location inaccuracy of sensor s_1 since the range-constraint $R_{t'}(x_c, y_c)$ cannot reduce the area of $ER_{s_1,t}$. Similarly, the range-constraint $R_{t'}(x_c, y_c)$ cannot help in improving the estimative regions of sensors s_2 and s_3. On the contrary, if mobile anchor moves along path p_1 and broadcasts a beacon at location $b = (x_b, y_b)$, the range-constraint $R_{t'}(x_b, y_b)$ significantly improves the location inaccuracies of sensors s_2 and s_3. As shown in Fig. 2, the resultant estimative regions of sensors s_2 and s_3 are $ER_{s_2,t}$ and $ER_{s_3,t}$, respectively. Compared with the $ER_{s_2,t}$ and $ER_{s_3,t}$, the new estimative regions are quite smaller than the original ones, hence contributing the maximal benefits for localization.

The benefits improved by sensors s_2 and s_3 can be calculated by

$$\begin{aligned} bef_{s_2,(x_b,y_b)} &= ER_{s_2,t} - ER_{s_2,t'} \\ bef_{s_3,(x_b,y_b)} &= ER_{s_3,t} - ER_{s_3,t'}. \end{aligned} \quad (6)$$

According to (3), (7) shows the total benefit obtained from the beacon $b(x_b, y_b)_{t'}$

$$bef_{(x_b,y_b)} = bef_{s_2,(x_b,y_b)} + bef_{s_3,(x_b,y_b)}. \quad (7)$$

This observation motivates us to investigate the anchor guiding mechanism for obtaining the maximal improvement on location inaccuracy of the WSN and minimizing the movement of the mobile anchor.

IV. The Guiding Mechanism

This section presents the proposed guiding mechanism for mobile anchor to contribute the maximal benefits for localization. The guiding mechanism mainly consists of four phases: *Identifying Promising Region Phase* (*IPRP*), *Weighting Phase* (*WP*), *Beacon Locations Selection Phase* (*BLSP*), and *Path Construction Phase* (*PCP*). The first phase, called *Identifying Promising Region Phase* (*IPRP*), aims to analyze the relation between the estimative regions and the communication ranges of static sensors, and thereby the *promising region* of each sensor can be determined. Then, the *Weighting Phase* (*WP*) partitions the promising region into a number of regular grids and determines the weight of each grid. Third, according to the weight of each grid, the *Beacon Locations Selection Phase* (*BLSP*) selects some of the most promising grids where the mobile anchor broadcasts beacons at those locations can significantly contribute benefits for improving the location inaccuracy of the WSN. Herein, we notice that the selection of beacon locations should satisfy the minimal movement constraint. Hence, this phase also presents two policies to achieve different goals according to the requirement of localization in either minimizing or balancing the location inaccuracies of all sensors. Finally, the *Path Construction Phase* (*PCP*) creates the shortest path for passing through all promising grids determined in $BLSP$. The following details each phase of the proposed guiding mechanism.

1) Identifying Promising Region Phase (IPRP): This phase aims to identify the promising region of each sensor. A promising region of sensor s at time t, denoted by $PR_{s,t}$, is a rectangle region, where a mobile anchor broadcasting a beacon at any location of this region might improve location inaccuracy of sensor s.

A beacon can help sensor s recalculate its new estimative region [4]–[15] if sensor s can receive the beacon from mobile anchor. That is, the mobile anchor should be located within the communication range of sensor s. However, the mobile anchor only has the knowledge that sensor s falls in the estimative region $ER_{s,t} = [(x_{s,1}, y_{s,1}), (x_{s,2}, y_{s,2})]_t$. Since sensor s might be located at any point belonging to its estimative region $ER_{s,t}$, and the mobile anchor should fall in the communication range of sensor s, the promising region $PR_{s,t}$ will be determined by extending the boundaries of estimative region $ER_{s,t}$ with length r which is the communication range of sensor s. As shown in Fig. 3, the mobile anchor can determine the $PR_{s,t}$ whose boundaries is marked by solid rectangular region. As a result, the mobile anchor can simply determine $PR_{s,t}$ by applying the coordinates of left-up and right-down points of $ER_{s,t}$. Let coordinates $(x_{s,1}, y_{s,1})$ and $(x_{s,2}, y_{s,2})$ denote the locations of left-up and right-down points of $ER_{s,t}$, respectively, the $PR_{s,t}$ can be calculated by

$$PR_{s,t} = [(x_{s,1} - r, y_{s,1} - r), (x_{s,2} + r, y_{s,2} + r)]_t. \quad (8)$$

However, the promising region might include a *helpless region* that the new range-constraint $R_{t'}(x_m, y_m)$ totally covers the $ER_{s,t}$ and hence cannot reduce the area size of $ER_{s,t}$. For example, as shown in Fig. 1, since the area size of $ER_{s,t'}$ is smaller than that of $ER_{s,t}$, the location inaccuracy of sensor s can be improved. Nevertheless, if the estimative region $ER_{s,t}$ is fully covered by the new range-constraint $R_{t'}(x_m, y_m)$, the new estimative region $ER_{s,t'}$ will be $ER_{s,t} \cap R_{t'}(x_m, y_m) = ER_{s,t}$. As a result, the location inaccuracy of sensor s cannot be improved by beacon $b(x_m, y_m)_{t'}$. The following gives the formal definition of helpless region and uses the Fig. 4 to illustrate how to determine the helpless region of each sensor.

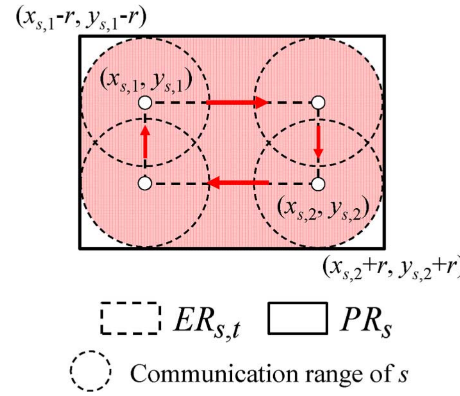

Fig. 3. *Promising region* of sensor s can be determined by the constraint that the mobile anchor is located within the communication range of sensor s.

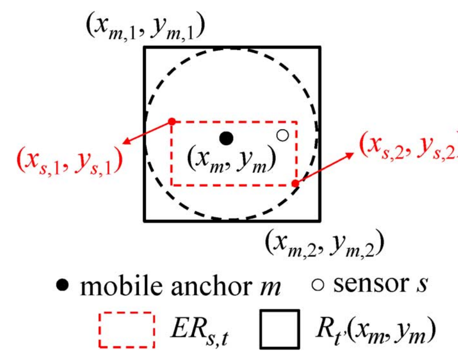

Fig. 4. Condition that $ER_{s,t}$ is fully covered by $R_{t'}(x_m, y_m)$ is necessary for deriving the $HLR_{s,t}$. That is, (9), (10), (11), and (12) hold.

The helpless region of sensor s is the region where mobile anchor located at any location within the region to broadcast a beacon cannot improve the location inaccuracy of sensor s. That is, the new range-constraint created by mobile anchor will fully cover sensor s's estimative region. Thus, if the mobile anchor can evaluate the helpless region, it should not broadcast the beacon in that region. Fig. 4 shows an example of the helpless region of sensor s at time t, denoted by $HLR_{s,t}$. Let the coordinates of left-up point and right-down point of $ER_{s,t}$ are $(x_{s,1}, y_{s,1})$ and $(x_{s,2}, y_{s,2})$, respectively. Let the location of mobile anchor be (x_m, y_m) and the coordinates of left-up point and right-down point of $R_{t'}(x_m, y_m)$ are $(x_{m,1}, y_{m,1})$ and $(x_{m,2}, y_{m,2})$, respectively. The $HLR_{s,t}$ can be easily calculated based on the information of the five coordinates. In case that the rectangle region $R_{t'}(x_m, y_m)$ fully covers the region $ER_{s,t}$, the intersection operation as depicted in (1) will equal to the original region $ER_{s,t}$, resulting that the beacon is helpless to improve the location inaccuracy of sensor s. Therefore, the condition that $ER_{s,t}$ is fully covered by $R_{t'}(x_m, y_m)$ is necessary for deriving the $HLR_{s,t}$. That is to say, (9), (10), (11), and (12) hold

$$x_{m,2} \geq x_{s,2} \tag{9}$$
$$y_{m,2} \geq y_{s,2} \tag{10}$$
$$x_{m,1} \leq x_{s,1} \tag{11}$$
$$y_{m,1} \leq y_{s,1}. \tag{12}$$

In addition, since the communication range of mobile anchor is r, we have the following:

$$x_{m,2} = x_m + r \tag{13}$$
$$y_{m,2} = y_m + r \tag{14}$$
$$x_{m,1} = x_m - r \tag{15}$$
$$y_{m,1} = y_m - r. \tag{16}$$

By substituting (13) to (9) and (14) to (10), respectively, (17) and (18) can be derived

$$x_m + r \geq x_{s,2} \Rightarrow x_m \geq x_{s,2} - r \tag{17}$$
$$y_m + r \geq y_{s,2} \Rightarrow y_m \geq y_{s,2} - r. \tag{18}$$

Similarly, by substituting (15) to (11) and (16) to (12), respectively, we have

$$x_m - r \leq x_{s,1} \Rightarrow x_m \leq x_{s,1} + r \tag{19}$$
$$y_m - r \leq y_{s,1} \Rightarrow y_m \leq y_{s,1} + r. \tag{20}$$

Then, after combining the (17) and (19) as well as (18) and (20), respectively, the following can be derived:

$$x_{s,2} - r \leq x_m \leq x_{s,1} + r \tag{21}$$
$$y_{s,2} - r \leq y_m \leq y_{s,1} + r. \tag{22}$$

Equations (21) and (22) determine the helpless region of sensor s. Based on (21) and (22), the $HLR_{s,t}$ can be represented by

$$HLR_{s,t} = [(x_{s,2} - r, y_{s,2} - r), (x_{s,1} + r, y_{s,1} + r)]_t. \tag{23}$$

As a result, the $PR_{s,t}$ should exclude the helpless region $HLR_{s,t}$. Equation (24) reflects this fact

$$\begin{aligned} PR_{s,t} &= PR_{s,t} - HLR_{s,t} \\ &= [(x_{s,1} - r, y_{s,1} - r), (x_{s,2} + r, y_{s,2} + r)]_t \\ &\quad - [(x_{s,2} - r, y_{s,2} - r), (x_{s,1} + r, y_{s,1} + r)]_t. \end{aligned} \tag{24}$$

2) Weighting Phase (WP): This phase aims at partitioning the whole monitoring region into a number of regular grids and proposes a weighting system that assigns each grid with a weight to represent the benefit obtained by broadcasting a beacon at each grid. A virtual coordinates system can be constructed for the grid-based WSN. Let $g(x, y)$ denote the grid located at the x_{th} row and y_{th} column of grids. Each grid $g(x, y)$ of PR_s will be locally assigned with a weight value according to the contribution to the location inaccuracy of sensor s if a beacon is broadcasted at that grid. The weight value assigned in grid $g(x, y)$ is called *Grid Benefit* of $g(x, y)$ (or $GB_{g(x,y)}$), which will be used

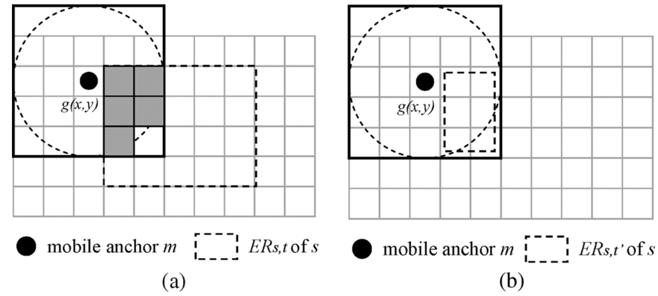

Fig. 5. (a) Gray area represents the possible locations of sensor s that mobile anchor m can communicate with sensor s. (b) New estimative region $ER_{s,t'}$, denoted by the dotted rectangle, is evaluated according to the new range-constraint.

to guide the mobile anchor for maximizing the total benefit of the anchor's movement. Any grid located out of the promising region of sensor s is assigned with zero value because there is no contribution to the location inaccuracy of sensor s.

Let $p_{s,g(x,y)}$ and $bef_{s,g(x,y)}$ denote the probability that the mobile anchor is within the communication range of sensor s and the improvement of location inaccuracy of sensor s, respectively. Since the $bef_{s,g(x,y)}$ can be measured by the difference of $ER_{s,t}$ to $ER_{s,t'}$, the $GB_{g(x,y)}$ to sensor s can be determined by

$$\begin{aligned} GB_{s,g(x,y)} &= p_{s,g(x,y)} \times bef_{s,g(x,y)} \\ &= p_{s,g(x,y)} \times (ER_{s,t} - ER_{s,t'}). \end{aligned} \tag{25}$$

Let $N_c(R)$ be the number of grids that mobile anchor located at those grids can communicate with sensor s in region R. Let $N_e(R)$ be the number of grids in region R. Then, the $GB_{s,g(x,y)}$ can be calculated by

$$\begin{aligned} GB_{s,g(x,y)} &= p_{s,g(x,y)} \times bef_{s,g(x,y)} \\ &= \frac{N_c(ER_{s,t'})}{N_e(ER_{s,t})} \times N_e(ER_{s,t} - ER_{s,t'}). \end{aligned} \tag{26}$$

The *Grid Benefit* of grid $g(x, y)$ is the summation of all benefits assigned by those sensors that grid $g(x, y)$ commonly belongs to their promising region. Let N denote the set of sensor nodes in the monitoring region. Equation (27) calculates the *Grid Benefit* of grid $g(x, y)$.

$$GB_{g(x,y)} = \sum_{\forall s \in N, \forall g(x,y) \in PR_s} GB_{s,g(x,y)} \tag{27}$$

Fig. 5 shows an example to illustrate the calculation of $GB_{s,g(x,y)}$. In the following, we assume that the mobile anchor broadcasts a beacon at grid $g(x, y)$ and discuss the contribution of this beacon to sensor s. In Fig. 5(a), the new range-constraint is depicted by the solid rectangle and the original estimative region $ER_{s,t}$ of sensor s is represented by the dotted rectangle. Since sensor s is possibly located at any grid of $ER_{s,t}$, the gray region marked in Fig. 5(a) represents those grids that are within the communication range of the mobile anchor located at $g(x, y)$. Therefore, $N_c(ER_{s,t})$ is 5 (the number of grids in the gray region). Since the number of grids in $ER_{s,t}$ is $N_e(ER_{s,t}) = 4 \times 5 = 20$, we have $p_{s,g(x,y)} = 5/20$ which indicates the probability that the mobile anchor located at grid

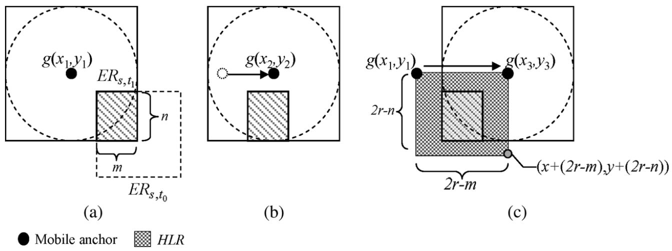

Fig. 6. (a) Mobile anchor broadcasts a beacon at grid $g(x_1, y_1)$ so that a new estimative region ER_{s,t_1} of sensor s has been formed. (b) A new range-constraint which constructed by mobile anchor at grid $g(x_2, y_2)$ will totally cover the ER_{s,t_1}. (c) The shadow region shows the new helpless region formed due to the change of ER of s from ER_{s,t_0} to ER_{s,t_1}.

$g(x, y)$ can communicate with sensor s. In case the sensor receives the mobile anchor's beacon, it applies (1) and calculates its new estimative region $ER_{s,t'}$ represented by the dotted rectangle as shown in Fig. 5(b). The number of grids in $ER_{s,t'}$ is 6. Therefore, the $bef_{s,g(x,y)}$ is $20 - 6 = 14$ grids. Then, the benefit of grid $g(x, y)$ can be calculated by

$$GB_{s,g(x,y)} = p_{s,g(x,y)} \times bef_{s,g(x,y)} = 0.25 \times (20 - 6) = 3.5.$$

Notice that one grid might belong to more than one promising regions. In other words, a beacon broadcasted at grid $g(x, y)$ might improve the location inaccuracies of several sensors. To aggregate all benefits of the same grid, each sensor s in the monitoring region should transfer its ER_s and $GB_{s,g(x,y)}$ to mobile anchor, for all $g(x, y) \in PR_s$. After obtaining the estimative regions and the corresponding grid benefits from all sensors, the mobile anchor will create a record for each grid of the monitoring region for storing its Grid Benefit. Each record of Grid Benefit consists of *Total_GB* and many *Each_GB* fields. If the mobile anchor broadcasting a beacon at grid $g(x, y)$ can improve the location inaccuracy of sensor s, the set $\{\text{sensor } s, GB_{s,g(x,y)}\}$ will be appended in the *Each_GB* field and the value of $GB_{s,g(x,y)}$ will be added into the*Total_GB* field. Finally, the *Total_GB* field maintains the value of $GB_{g(x,y)}$ for each grid $g(x, y)$.

3) Beacon Locations Selection Phase (BLSP): In this phase, the mobile anchor selects beacon locations for obtaining maximal benefits in executing localization task. First of all, we would like to present a concept that any two beacon locations should be far away from each other at certain distance. Let the mobile anchor broadcast a beacon at grid $g_t(x, y)$ at time t and then broadcast another beacon at grid $g_{t'}(x, y)$ at time t' with a certain distance, as shown in Fig. 6. Let the new range-constraint improve the location inaccuracy of sensor s. We observe that the area of helpless region of sensor s will be changed and increased with the size of $ER_{s,t}$. The new helpless region should be derived so that the mobile anchor can select the beacon location outside the helpless region.

The following presents how the mobile anchor determines the new helpless region. As shown in Fig. 6(a), ER_{s,t_0} is denoted by the dotted rectangle. When a mobile anchor broadcasts a beacon at grid $g(x_1, y_1)$ at time t_1, the ER_{s,t_0} is changed to ER_{s,t_1} that is sized $m \times n$. In Fig. 6(b), mobile anchor moves from $g(x_1, y_1)$ to $g(x_2, y_2)$ with a certain distance. The new range-constraint cannot improve the location inaccuracy of sensor s. In Fig. 6(c), the shadow region shows the new helpless region formed due to the change of ER of s from ER_{s,t_0} to ER_{s,t_1}. This indicates that the beacon broadcasted at any location of the shadow region will form a new range-constraint which will totally cover the ER_{s,t_1}. The width and length of the new helpless region are $2r - m$ and $2r - n$, respectively. Therefore, assume that the new ER_{s,t_1} has been constructed by sensor s because of receiving a beacon from mobile anchor at location $g(x_1, y_1)$ at time t_1. Equation (28) gives the evaluation of the new helpless region.

$$HLR_{s,t_1} = [(x_1, y_1), (x_1 + (2r - m), y_1 + (2r - n))]_{t_1} \tag{28}$$

This study proposes two policies, called *benefit-based* and *distance-based selection policies*, for mobile anchor selecting beacon locations. The following presents the two selection policies. Let G denote the set of selected grids for broadcasting beacons. Let S_i denote the set of sensors whose sizes of estimative regions can be reduced if the mobile anchor broadcasts a beacon at grid $g(x_i, y_i)$. The ER_{s_i} denotes the set of new estimative regions of sensors belonging to set S_i after these sensors receiving the beacon broadcasted at grid $g(x_i, y_i)$. Furthermore, let HLR_{s_i} denote the set of new formed helpless regions derived according to the ER_{s_i}.

A. Benefit-Based Selection Policy

The *Benefit-Based Selection* (*BBS*) policy aims at maximizing the benefits in executing the localization task. That is, the BBS scheme selects one grid that has optimum benefit at a certain time. It only considers those grids whose benefit values are larger than the predefined benefit threshold σ. Herein, we notice that the benefit threshold σ is a user defined value. The smaller value of σ represents the larger number of beacon locations, leading to a longer path length and higher energy consumption for the mobile anchor. In the Performance Study section, the value of σ is set to 10. Let there be k grids $g(x_i, y_i)$, $1 \le i \le k$, satisfying

$$GB_{g(x_1,y_1)} \ge GB_{g(x_2,y_2)} \ge \cdots \ge GB_{g(x_k,y_k)} \ge \sigma. \tag{29}$$

The following gives the BBS procedure.

Benefit-Based Selection Procedure

Input: grid $g(x_i, y_i)$

Output: beacon locations

```
G = {g(x_1, y_1)}; HLR = {HLR_{s_i}}
FOR i = 2 to k {
   IF (g(x_i, y_i) ∉ HLR)
      G = G ∪ {g(x_i, y_i)}
      HLR = HLR ∪ {HLR_{s_i}}
   END IF
END FOR
```

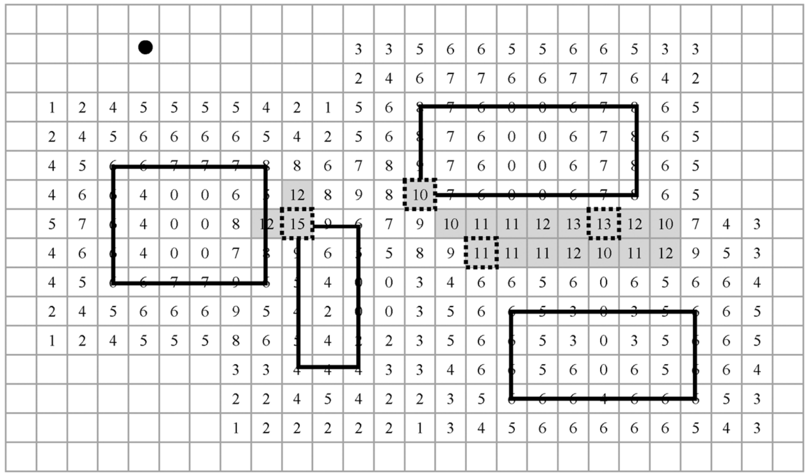

Fig. 7. An example of applying the *Benefit-Based Selection* policy to select grids for broadcasting beacons.

Initially, in line 1, the first grid $g(x_1, y_1)$ that has the highest priority is selected in set G. Since the new grid $g(x_1, y_1)$ is selected, this implies that there is a new beacon broadcasted at grid $g(x_1, y_1)$. The new beacon will construct one or more new estimation regions, which result in a new helpless region set called HLR. Therefore, the new helpless region set HLR should be recalculated to avoid the subsequently selected grids falling in HLR. Line 2 checks whether or not the subsequent $k-1$ grids can be selected in G. In line 3, if the considered i-th grid $g(x_i, y_i)$ does not fall in the new helpless region set HLR, it is selected in set G, as shown in line 4. Line 5 recalculates the new helpless region set HLR according to (28).

Fig. 7 is an example illustrating the BBS policy. Each solid square represents the current estimative region of each sensor. The threshold is set to 10 in this example. Therefore, those grids that are marked with gray color are considered as the candidates for broadcasting the beacons. Initially, the grid with maximum benefit 15 is selected. Then the grid with the second highest benefit 13 is considered. Since this grid does not belong to the helpless region of any sensor, it is selected and is included in set G. The next grid will be selected if it has the maximal benefit among the unchecked grids and it does not belong to the set of helpless regions. As a result, the selected grids are marked with dotted squares as shown in Fig. 7.

B. Distance-Based Selection Policy

The *Distance-Based Selection* (*DBS*) policy aims at minimizing the moving distance and thus saves the energy consumption in executing the localization task. The *DBS* policy selects the next grid that has minimal distance to the current selected grid. Let mobile anchor m be located at grid $g(x_m, y_m)$ currently. Let there be k grids $g(x_i, y_i) \geq \sigma, 1 \leq i \leq k$, that satisfy $dist(g(x_m, y_m), g(x_1, y_1)) \leq dist(g(x_m, y_m), g(x_2, y_2)) \leq \ldots \leq dist(g(x_m, y_m), g(x_k, y_k))$, where $dist(g(x_m, y_m), g(x_i, y_i))$ denotes the distance between grids $g(x_m, y_m)$ and $g(x_i, y_i)$. The DBS algorithm is the same as BBS algorithm except that it selects grids according to the distances of the selected grids. The following gives the DBS procedure.

Distance-Based Selection Procedure

Input: grid $g(x_i, y_i)$

Output: beacon locations

$L = \{g(x_2, y_2), g(x_3, y_3), \ldots, g(x_k, y_k)\}$; $r = 1$

$HLR = \{HLR_{s_i}\}$

WHILE ($L \neq \emptyset$)

  Let $DIS(r, t) = \min_{1 \leq s \leq k} DIS(r, s)$, where $r \neq t$ and $g(x_s, y_s) \in L$

  $G = G \cup \{g(x_t, y_t)\}$

  $HLR = HLR \cup \{HLR_{s_j}\}$

  $L = L - \{g(x_t, y_t)\}$; $r = t$

END WHILE

Let L denote the set of remaining candidates for beacon locations. The mobile anchor m initially selects $g(x_1, y_1)$. Then it treats the selected grid $g(x_1, y_1)$ as $g(x_m, y_m)$ and repeats the DBS selection operations until $L = \{\emptyset\}$. Let $d_{i,j}$ denote the value of entry $DIS_{k \times k}(i, j)$ which represents the distance between grids $g(x_i, y_i)$ and $g(x_j, y_j)$, for $1 \leq i, j \leq k$. The following gives the DBS procedure. Since the $g(x_1, y_1)$ is selected for being a beacon location, the DBS algorithm looks the first row ($r = 1$) of DIS matrix to find the grid with minimal distance to $g(x_1, y_1)$. We assume that entry $DIS(r, t)$ has a minimum value in row r. Therefore, the grid $g(x_t, y_t)$ will be selected. This indicates that the mobile anchor will broadcast a beacon at grid $g(x_t, y_t)$. Then, the DBS procedure will further select the next grid by checking the t-th row, which records the distances of grid $g(x_t, y_t)$ to other grids. The WHILE loop will be terminated once all grids in set L have been checked.

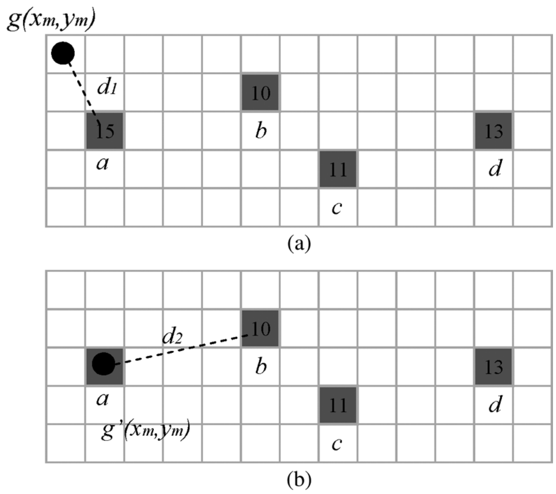

Fig. 8. An example for illustrating the PCP phase. (a)The edge connecting $g(x_m, y_m)$ and a is constructed. (b) Another edge that connects grids a and b is constructed.

1) Path Construction Phase (PCP): This phase presents how the mobile anchor constructs the path that passes through those beacon locations selected in the $BLSP$. The path construction aims at obtaining maximal benefits and minimizing the movement in executing the localization task. The energy consumption of the mobile anchor, say E_m, will be evaluated in the phase. Let mobile anchor m moving for a path length $|p|$ and having i turns and k stops for broadcasting beacons during the movement consume $E_m = |p| \times e_p + k \times (e_{\text{stop}} + e_{\text{beacon}}) + i \times e_{\text{turn}}$. Let G be the set of the grids selected from $BLSP$ and $g(x_m, y_m)$ be the current grid location. Let P denote the constructed path which starts at $g(x_m, y_m)$ and ends at $g(x_e, y_e)$. Let $EG_{a,b}$ denote the edge which starts at $g(x_a, y_a)$ and ends at $g(x_b, y_b)$. The constructed path will be extended by connecting as many new edges as possible. Note that each extended edge will have maximal benefit-cost ratio so that the total improvement of location inaccuracy is optimal. The following gives the PCP algorithm.

Fig. 8 shows an example illustrating the PCP phase. As shown in Fig. 8(a), assume that there are four grids a, b, c and d selected in the $BLSP$ phase and they have benefits 15, 10, 11 and 13, respectively. In the path construction phase, mobile anchor m is located at the grid $g(x_m, y_m)$. We assume $15/dist(g(x_m, y_m), a) > 10/dist(g(x_m, y_m), b) > 11/dist(g(x_m, y_m), c) > 13/dist(g(x_m, y_m), d)$. Therefore, the mobile anchor constructs the edge connecting grids $g(x_m, y_m)$ and a, as shown in Fig. 8(a). The energy consumption for moving from $g(x_m, y_m)$ to a is evaluated. Then PCP algorithm continues executing the next WHILE loop and compares the values of ratios $10/dist(a, b)$, $11/dist(a, c)$, $13/dist(a, d)$. As shown in Fig. 8(b), the edge connecting grids a and b is constructed in the path and the energy consumption for moving from $g(x_m, y_m)$ to b passing through a is evaluated. Similar operations will be executed by mobile anchor for constructing a path that obtains as many benefits as possible under the energy constraint E_c.

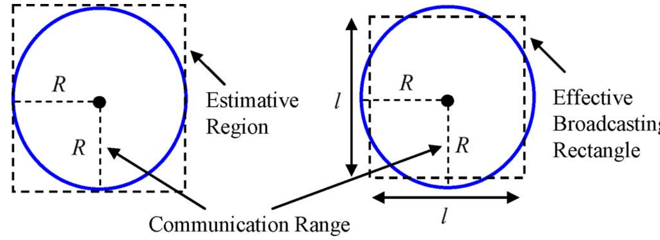

Fig. 9. The effective broadcasting rectangle can be treated as a rectangle region which has the effective communication area size as the circle region.

Path Construction Phase Algorithm (PCP)

Input: beacon locations

Output: path P

$g(x_e, y_e) = g(x_m, y_m)$
$P = EG_{m,e}$; $E_m = 0$
Let $dist(EG_{e,i}) = dist(g(x_e, y_e), g(x_i, y_i))$
WHILE ($G \neq \emptyset$)
  $g(x_i, y_i) = \max\{GB_{g(x_i,y_i)}/dist(EG_{e,i})\}$, where $g(x_i, y_i) \in G$
  IF (($x_e = x_t$) or ($y_e = y_t$)) $turn = 0$
  ELSE $turn = 1$
  $P = P + EG_{e,t}$; $g(x_e, y_e) = g(x_t, y_t)$
  $E_m = E_m + (dist(EG_{e,t}) \times e_p) + e_{stop} + e_{beacon} + turn \times e_{turn}$
  $G = G - \{g(x_t, y_t)\}$
END WHILE

V. Analysis of the BBS Guiding

Let the communication range of all sensors are identical and equal to R. To simplify the analysis, the region of communication range is transferred to a certain rectangle region, called *effective broadcasting rectangle* (*EBR*), whose size equals to that of communication range. Let the region size of *effective broadcasting rectangle* be $l \times l$, where $l = \sqrt{\pi}R$, as shown in Fig. 9.

Recall that the proposed *Benefit-Based Selection* (*BBS*) policy aims at maximizing the benefits in executing the localization task. In the analysis, we aim to compare the total movement distance of the mobile anchor by applying the existing *snake-like* mechanism and the proposed BBS policy, under the constraint that both of them satisfy the same required location inaccuracy.

To compare the total movement distance of the mobile anchor by applying the existing snake-like mechanism and the proposed guiding mechanism using BBS policy, we further partition each EBR into a number of grids and the area size of each grid is $d \times d$, as shown in Fig. 10. Hence, the area size of the estimative region of each sensor can be evaluated by the number of grids

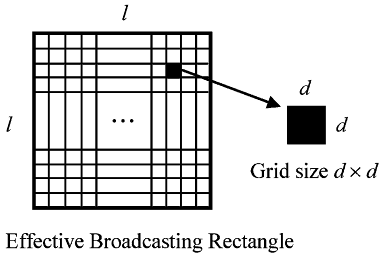

Fig. 10. The effective broadcasting rectangle of the sensors is partitioned into the grids with the size of $d \times d$.

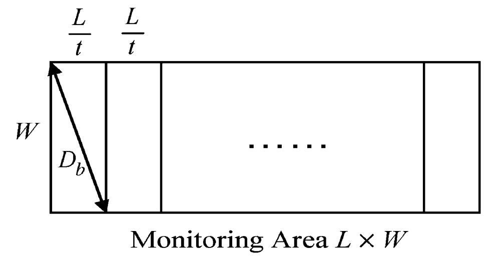

Fig. 11. Applying the BBS policy, the anchor will move and beacon t times and the moving distance for each beacon is D_b in the worst case.

and the total number of grids in each EBR can be denoted by l^2/d^2.

Let λ denote the average number of grids in the estimative region of each sensor after applying the proposed BBS policy. The smaller value of λ represents that the estimative region is smaller, leading to a lower location inaccuracy. Hence, if a scheme is able to achieve a smaller value λ for each estimate region, the scheme has higher performance for localization. Recall that the area size of EBR is $l \times l$. The area size of the estimative region of each sensor after applying the proposed BBS policy will be λd^2 while the eliminated area size of the estimative region of each sensor from the EBR after applying the proposed BBS policy will be $l^2 - \lambda d^2$. Let *required location Accuracy* (*RLA*) be a user predefined value and be defined by $(l^2 - \lambda d^2)/l^2$, as shown in

$$RLA = \frac{l^2 - \lambda d^2}{l^2}. \tag{30}$$

The larger value of numerator of RLA represents that the estimative region is reduced more significantly. Therefore, if a scheme achieves higher RLA, the scheme is with higher localization performance.

Let $RLA = 1 - \delta$, where $0 \leq \delta \leq 1$. The constraint of the grid size, d, can be derived as shown in

$$\begin{aligned} RLA &= \frac{l^2 - \lambda d^2}{l^2} = 1 - \delta \Rightarrow d^2 = \frac{\delta l^2}{\lambda} \\ &\Rightarrow d = \sqrt{\frac{\delta l^2}{\lambda}} = \frac{\sqrt{\delta \pi R^2}}{\sqrt{\lambda}} = \frac{\sqrt{\delta \pi} R}{\sqrt{\lambda}}. \end{aligned} \tag{31}$$

For example, the value of RLA is set to 0.9, where δ is 0.1. We set 1-δ for the value of RLA but not δ since it is able to simplify (31). This also indicates that the grid size has an upper bound if a certain location accuracy 1-δ is required. Since the small grid size will increase the movement distance in the BBS policy, the maximal value of d will be considered in the analysis to reduce the movement distance while the predefined RLA constraint can be satisfied.

As shown in (32). let L and W denote the length and width of the given monitoring area. Herein, we assume that $L = kW$ since the length L can be represented as k times of width W where $k \geq 1$ is a constant value

$$W = eR = \frac{e\sqrt{\lambda}}{\sqrt{\pi\delta}} d, \text{ and } L = kW = \frac{ke\sqrt{\lambda}}{\sqrt{\pi\delta}} d. \tag{32}$$

Let the average benefit of each beacon be u grids by applying the BBS policy and the number of the deployed static sensors in the monitoring region be n. Let g_{remove} denote the number of grids in each EBR that are removed from the anchor's beacons by applying the BBS policy. The g_{remove} can be evaluated by

$$g_{remove} = n\left(\frac{l}{d}\right)^2 - n\lambda. \tag{33}$$

Since each beacon contributes the average benefit of u grids by applying the BBS policy, the number of beacons, say t, required to achieve the requested location accuracy is shown in

$$\begin{aligned} t &= \left\lfloor \frac{g_{remove}}{u} \right\rfloor = \left\lfloor \frac{n\left(\frac{l}{d}\right)^2 - n\lambda}{u} \right\rfloor = \left\lfloor \frac{n\left(\frac{\lambda^2}{\delta}\right) - n\lambda}{u} \right\rfloor \\ &= \left\lfloor \frac{n\lambda(1-\delta)}{u\delta} \right\rfloor, \text{ where } d = \frac{\sqrt{\pi\delta}R}{\sqrt{\lambda}} \text{ and } l = \sqrt{\pi}R. \end{aligned} \tag{34}$$

Fig. 11 partitions the whole monitoring regions into t regular blocks. In the worst case, the mobile anchor by applying the BBS policy should move for a distance of D_b for each beacon, where D_b can be evaluated by

$$D_b \leq \sqrt{\frac{L^2}{t^2} + W^2} = \frac{W\sqrt{k^2 + t^2}}{t}. \tag{35}$$

The total movement distance, called D_{BBS}, of the BBS policy is computed by

$$D_{BBS} = tD_b \leq W\sqrt{k^2 + t^2}. \tag{36}$$

Assume that the compared scheme, *Snake-Like*, guides the anchor grid by grid following the directions from up to down and from left to right. As a result, the performance improvement of BBS policy against the *Snake-Like* policy in terms of total movement distance can be estimated as

$$\begin{aligned} \frac{D_{snake-like}}{D_{BBS}} &\geq \frac{\frac{L}{d} \times \frac{W}{d} \times d + L}{W\sqrt{k^2+t^2}} = \frac{L(\frac{W}{d}+1)}{W\sqrt{k^2+t^2}} = \frac{k(W+d)}{d\sqrt{k^2+t^2}} \\ &= \frac{kd\left(\frac{e\lambda}{\sqrt{\pi\delta}}+1\right)}{d\sqrt{k^2+t^2}} \geq \frac{ke\lambda}{\sqrt{\pi\delta}\sqrt{k^2+t^2}} \\ &\geq \frac{ke\lambda}{\sqrt{\pi\delta}\sqrt{(k+t)^2}} = \frac{ke\lambda}{\sqrt{\pi\delta}(k+t)} \qquad (37) \\ &= \frac{ke\lambda}{\sqrt{\pi\delta}\left(k + \left\lfloor \frac{n\lambda(\lambda-\delta)}{u\delta} \right\rfloor\right)} \qquad (38) \\ &\geq \frac{ke}{\sqrt{\pi\delta}\left(k + \left(\frac{n(1-\delta)}{u\delta}\right)\right)}, \text{ when } \lambda = 1. \qquad (39) \end{aligned}$$

By applying the *Snake-Like* scheme, the mobile anchor broadcasts the beacon grid by grid and thus the average number of grids included in the estimative region of each sensor will be reduced to 1. To the ease of comparison, the value of λ in BBS is also set to 1. As a result, (38) will be simplified to (39). In (39), when the values of e, δ, n and k are constant, the performance improvement of the proposed BBS compared to the *Snake-Like* will increase with the value of u. This also verifies the key idea of the proposed BBS policy that BBS aims to maximize the benefit of each beacon and hence minimize the anchor's movement.

In addition, if the grid size is smaller than a threshold, (37) can be further simplified to conclude that the proposed BBS approach outperforms *Snake-Like* approach in terms of moving distance. More specifically, let condition $L/t > d$ be satisfied. This condition indicates that the average moving distance in horizontal direction in the BBS policy is greater than that of the *Snake-Like* policy. Furthermore, it also means that each beacon of the BBS policy can obtain greater average benefits than that of the *Snake-Like* policy if the moving distance of the BBS policy is longer than that of the *Snake-Like* policy in horizontal direction. Since $L = kW$ and $k \geq 1$, (37) can be further simplified to (40) which indicates that the moving distance of the proposed BBS will be shorter than the *Snake-Like* approach. This guarantees that the result presented in (40) is always valid for a rectangle monitoring region

$$\begin{aligned} &\text{When } \frac{L}{t} > d, \quad t < \frac{L}{d} \\ &\frac{D_{snake-like}}{D_{BBS}} \geq \frac{k(W+d)}{d\sqrt{k^2+t^2}} > \frac{k(W+d)}{d\sqrt{k^2+\left(\frac{kW}{d}\right)^2}} \\ &\qquad = \frac{k(W+d)}{k\sqrt{d^2+W^2}} \geq \frac{k(W+d)}{k\sqrt{(d+W)^2}} = 1 \\ &\qquad \therefore \frac{D_{snake-like}}{D_{BBS}} > 1. \end{aligned} \tag{40}$$

VI. Performance Study

This section compares the performance results of the proposed *Anchor-Guiding Mechanism* (*AGM*) with the *Snake-Like* [14], [15] and *Random* movements [3] using the Glomosim simulator [16]. The GloMoSim simulator is a library-based sequential and parallel simulator for wireless networks. The major reason for us to select GloMoSim as our simulator is that our proposed guiding mechanism and the compared approaches can be simply programmed using PARSEC language which is a C-based parallel simulation language. We use GloMoSim simulator to investigate the performance results in terms of the impact of network density and localization time on location inaccuracies (described in Section VI-A1), the impact of energy consumption and thresholds on location inaccuracies (described in Section VI-A2) as well as the impact of energy consumption and thresholds on balance index (described in Section VI-A3).

In the simulation study, the benefit-based and distance-based anchor-guiding policies applied in AGM are denoted by $BB-AGM$ and $DB-AGM$, respectively. In executing the *Snake-Like* and *Random* movements, the time-based and distance-based policies are applied for mobile anchor to determine when or where a beacon should be broadcasted. In *Random* movements, the mobile anchor broadcasts a beacon every time unit. Let β denote the distance of two parallel trajectories of the *Snake-Like* movement. The value of β is set at 2 and 4 to observe its impact on the performance of *Snake-Like* movement.

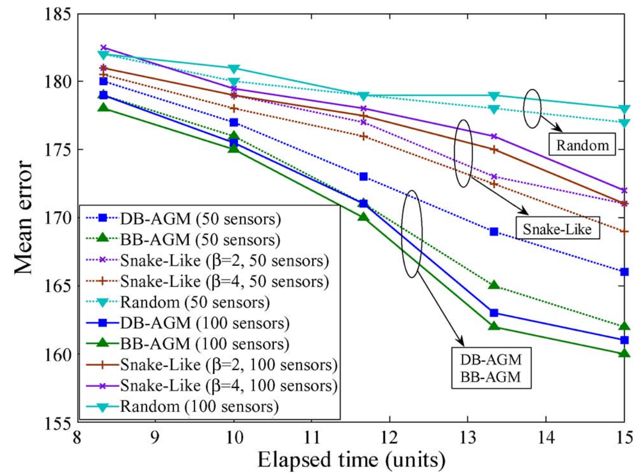

Fig. 12. Impact of network density and time spent for localization on the location error.

The network environment is described below. The size of the monitoring region is 300 units $\times$ 300 units. A number of static sensors, ranging from 20 to 100, are randomly deployed in the WSN. The monitoring region is partitioned into 300 $\times$ 300 grids. The communication radius is 10 units. The mobile anchor is located at the left-up corner of the monitoring region and moves at a constant speed and stops to broadcast a beacon for localization. The energy consumptions required for constant-speed movement for a unit distance, broadcasting a beacon, making a turn, and stop-then-start are 0.98 W, 0.017 W, 3 W, and 0.7 W, respectively.

1) The Impact of Network Density and Localization Time on Location Inaccuracies: In literature, many location-aware applications highly rely on each sensor's accurate location, rather than on an estimative region. To fit the existing applications, the estimation region of each sensor should be transferred to an estimate location. The estimate location of sensor s, denoted by (x_{est}, y_{est}), is the cross point of the two diagonal lines of ER_s. The location error of a sensor s can be measured by

$$P_{error,s} = \sqrt{(x_{est} - x_{real}) + (y_{est} - y_{real})^2} \tag{41}$$

where (x_{real}, y_{real}) is the real location of sensor s. Hence, the mean location error of the WSN can be derived by

$$P_{error} = \left(\sum_{i=1}^{n} P_{error,s_i}\right) / n \tag{42}$$

where n denotes the number of static sensors deployed over the monitoring region.

Fig. 12 measures the impact of network densities and the time spent for localization on the location error. All mechanisms have a common feature. When the network density is fixed, the mean location error decreases with the localization time. However, the proposed anchor-guiding approaches $DB-AGM$ and $BB-AGM$ outperform the *Snake-like* and *Random* movement mechanisms in terms of mean location error in all cases of the network density and the localization time. When the mean location error and network density are fixed, the proposed approaches require shorter localization time than the other two mechanisms. This is because the approaches of the proposed $DB-AGM$ and $BB-AGM$ guide the mobile anchor along the path that passes through the most promising locations for broadcasting beacons.

Fig. 12 also depicts that the proposed approaches have lower mean error, especially in the case of high network density. The major reason is that the number of beacon locations increases with the number of sensors, which significantly improves the location inaccuracies of the sensors. On the other hand, the mean error of *Snake-like* mechanism increases with the network density. The trajectory and beacon locations of the *Snake-like* movement do not change with the network density. Therefore, the maximal path length that the mobile anchor could exert before its energy exhaustion will be a constant. However, the number of sensors that are not visited by the mobile anchor increases with the network density. Therefore, there are more sensors obtaining no location information in a higher network density, and hence the mean error of *Snake-like* movement mechanism increases. Moreover, a higher β value will result in a lower mean error by applying the *Snake-like* movement. The major reason is that a higher β value makes the beacon locations cover a larger area size, which results in a lower mean error. Regarding the *Random* movement mechanism, the trajectory of the mobile anchor's movement is randomly determined. When the network density is increased, the number of sensors that do not receive any beacon from mobile anchor increases, which results in a higher mean error.

2) The Impact of Energy Consumption and Thresholds on Location Inaccuracies: The location inaccuracy of sensor s at time t, noted as $LI_{s,t}$, is denoted the area size of estimative region $ER_{s,t}$. Hence, the unit of the location inaccuracy is square meters. The smaller size of $ER_{s,t}$ represents that sensor s has a smaller estimative region, which also indicates that the maximal distance from the real location of the sensor to any point in $ER_{s,t}$ is smaller.

Let $LI_{WSN,t}$ denote the location inaccuracy of WSN at time t and it can be measured by

$$LI_{WSN,t} = \sum_{i=1}^{n} LI_{s_i,t}. \quad (43)$$

A smaller value of $LI_{WSN,t}$ represents a lower location inaccuracy of WSN at time t. Therefore, the ratio of localization inaccuracy, called localization efficiency, of mobile anchor from time t to t' is measured by $1 - LI_{WSN,t'}/LI_{WSN,t}$. In the best case, each sensor has a location point at time t', implying that the value of $LI_{WSN,t'}$ is zero. In the worst case, the mobile anchor does not help to reduce the size of estimation region of any sensor and hence the value of $LI_{WSN,t'}/LI_{WSN,t}$ is equal to 1 and thus the localization efficiency is equal to zero. Therefore, the value of localization efficiency is normalized between zero and one, and a larger value indicates better localization efficiency.

Fig. 13 compares the localization efficiencies of the proposed approaches and the other two mechanisms under the constraint of the energy consumption for the anchor's movement. In

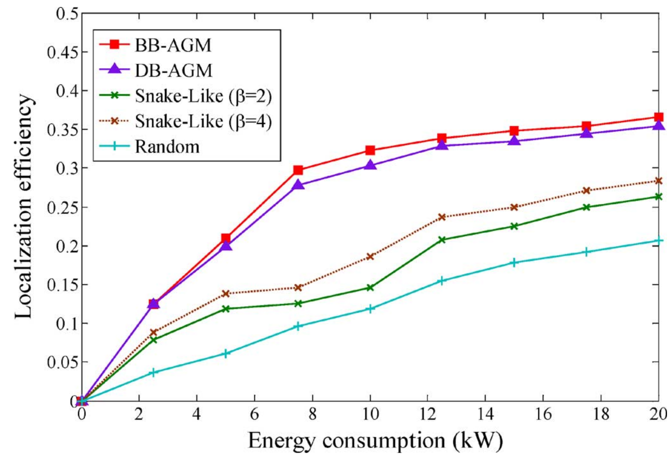

Fig. 13. $BB-AGM$ and $DB-AGM$ achieve higher localization efficiency than the other two mechanisms under the energy constraint.

general, the localization efficiency is increased with the number of beacons broadcasted by mobile anchor at the locations where can obtain higher benefit. However, the mobile anchor consumes more energy for its movements and broadcasting beacons. That is the major reason that the localization efficiency of static sensors is increased with the energy consumptions of the mobile anchor. As shown in Fig. 13, the proposed approaches have larger values than the *Snake-like* and *Random* movement schemes and thus outperform them in terms of localization efficiency. Moreover, $BB-AGM$ has a better performance than $DB-AGM$ because the benefit-based policy always guides the mobile anchor moving along the path that passes through the beacon locations for obtaining the maximal benefits in localization.

Fig. 13 also depicts another result that the proposed approaches consume much fewer energy than the other two mechanisms to meet the requirement of a given expected localization efficiency. On the other hand, the mobile anchor that applies the *Snake-like* movement with a larger β value will result in a wider spacing between any two parallel trajectories, which leads to a larger number of sensors receiving the anchor's beacons and hence results in better localization efficiency.

Let *mean error* is the mean location error of all sensors and is defined by the average square of the distance from the centers of all estimative regions to the actual locations of all sensors. Let ER_i be the estimative region of sensor s_i, where $1 \leq i \leq n$. Let (x_i', y_i') and (x_i, y_i) be the center location of ER_i and the actual location of sensor s_i. The mean error can be formulated by

$$\text{mean error} = \frac{1}{n}\sum_{i=1}^{n}\left((x_i' - x_i)^2 + (y_i' - y_i)^2\right). \quad (44)$$

The *Benefit-Based approach* (*BB-AGM*) may improve the location inaccuracies of those sensors whose sizes of estimative regions are bigger than the predefined threshold value α. Fig. 14 investigates the impact of threshold values on the anchor's energy consumption as well as the mean error. In case the mean error is fixed, the energy consumption of $BB-AGM$ decreases with the threshold value. A higher threshold value indicates that

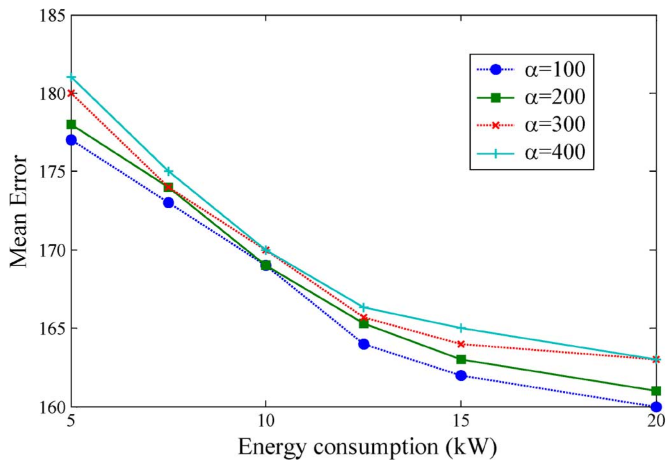

Fig. 14. Impact of threshold values on the anchor's energy consumption as well as the mean location error by applying the $BB-AGM$ approach.

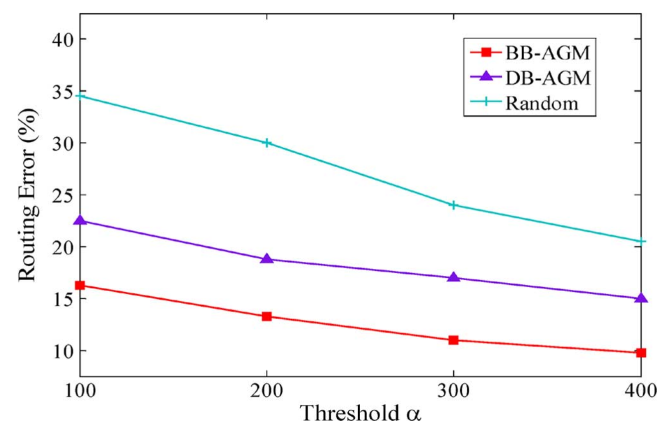

Fig. 15. Comparison of routing error of the proposed approaches and *Random* movement under various threshold values. The constraint of mobile anchor's remaining energy is set at 10 kW.

the number of sensors whose location inaccuracies are improved by mobile anchor is smaller, thereby saving the mobile anchor's power consumption.

Higher mean location errors may cause more routing error. In the experiments, the well known GPSR [17] is applied to construct routes from randomly selected sources to destinations. GPSR is one of the famous location-aware routing protocols [17]. By applying this routing protocol, the source node or forwarding node selects its neighboring sensor that is the closest to the destination node as the next data forwarder. This operation will be repeatedly executed until the data reaches the destination node.

Fig. 15 shows that $BB-AGM$ achieves lower routing error than $DB-AGM$ and *Random* movement since the benefit-based policy guides the mobile anchor to obtain the maximal benefits and thus reduces the mean location error in localization under energy constraint. Fig. 16 shows the snapshot obtained by applying the $BB-AGM$ approach on the WSN for 1000 time units. In Fig. 16, the hollow and solid nodes represent the estimate and real locations of sensors, respectively. Since the estimated location of each sensor is very close to real location,

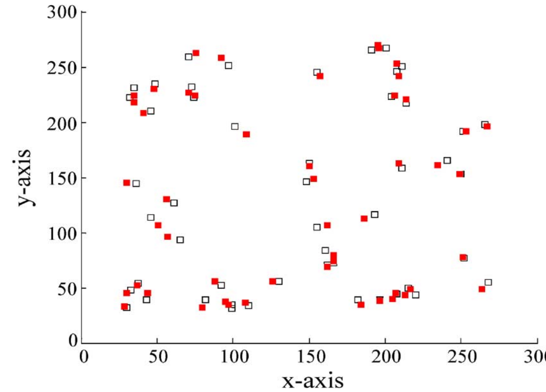

Fig. 16. Snapshot obtained by applying $BB-AGM$. The number of deployed sensors and α are set by 50 and 100, respectively.

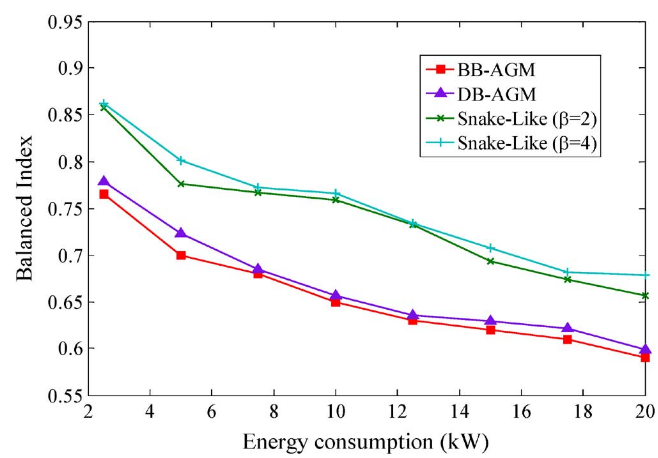

Fig. 17. $BB-AGM$ achieves better performance in terms of location inaccuracies of all sensors under the constraint of mobile anchor's remaining energy.

the proposed $BB-AGM$ effectively improves the location inaccuracies of all sensors in the monitoring region.

3) The Impact of Energy Consumption and Thresholds on Balance Index: In the experiments, a *Balanced Index* BI, as shown in (45), is used to measure the balance of the sensors' location inaccuracies

$$BI = \left(\sum_{i=1}^{n} \sum_{j=1}^{n} \left(|ER_{s_i}| - |ER_{s_j}| \right) \right) / \left(2n^2 |ER_{mean}| \right) \tag{45}$$

where the ER_{mean} denotes the mean value of the sizes of all sensors' estimative regions. A smaller value of BI indicates that the sizes of estimative regions of all sensors are likely equal.

Fig. 17 compares the proposed approaches with the *Snake-like* movement mechanism. All of the compared movements have a common feature that the BI value decreases with the energy consumption. The proposed approaches have a smaller value of BI and thus have a better performance in terms of balancing the location inaccuracies of the WSN. Moreover, the proposed $BB-AGM$ saves significant energy than $DB-AGM$ and *Snake-like* movement for achieving the same value of BI. The proposed $BB-AGM$ aims at moving to the grid with maximal broadcasting benefit. Hence, $BB-AGM$ has the best performance in terms of BI. Regarding the *Snake-Like* movement,

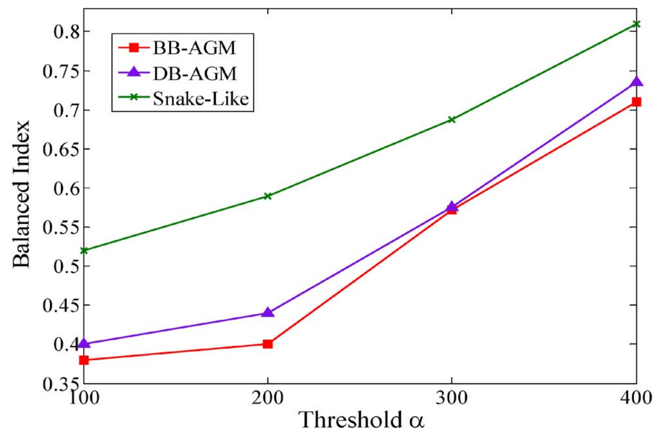

Fig. 18. Comparison of *Balance Index* of the proposed approaches and *Snake-like* movement under various threshold values where the constraint of mobile anchor's remaining energy is set at 10 kW.

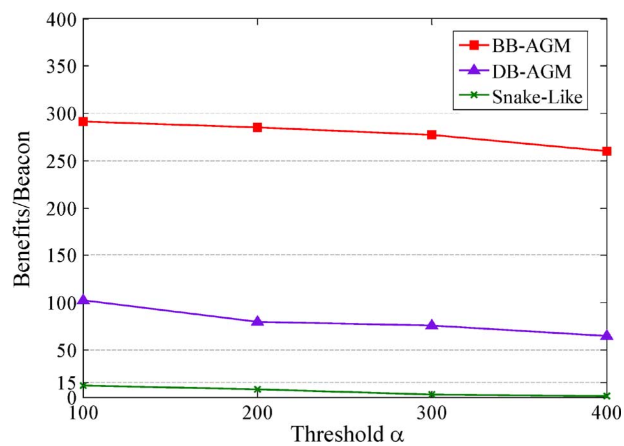

Fig. 19. Comparison of $BB-AGM$, $DB-AGM$, and *Snake-Like* in terms of beacon benefits by varying the value of α.

a higher β value causes a larger distance between two consecutive parallel trajectories. Therefore, more sensors will receive beacons from the mobile anchor and the BI will be reduced. Hence, the BI of *Snake-like* movement is decreased with the β value.

Recall that the threshold value α will constrain the mobile anchor only moving to those grids with the grid benefit higher than α. Fig. 18 investigates the impact of threshold value α on the BI for the proposed approaches and the *Snake-like* movement under considering that the mobile anchor has energy constraint. Obviously, the BI values of the compared movements decrease with the threshold value as shown in Fig. 18. It is because that a higher threshold value indicates a smaller number of sensors whose location inaccuracies are improved by mobile anchor. Let beacon benefit denotes the summation of grid benefits for those grids falling in the beacon range. Figs. 19 and 20 show the impacts of threshold value α on the beacon benefits for the three proposed approaches and the *Snake-like* movement under the same energy constraint considered in Fig. 18. Since the $BB-AGM$ aims at moving to the grid with maximal grid benefit, it has fewer impact by the value of α. However, applying the other three mechanisms will result in a larger distance between the visited grids and hence the mobile anchor consumes more energy for movement. As a result, the $BB-AGM$ approach outperforms the other three mechanisms in terms of the beacon benefits as shown in Fig. 19.

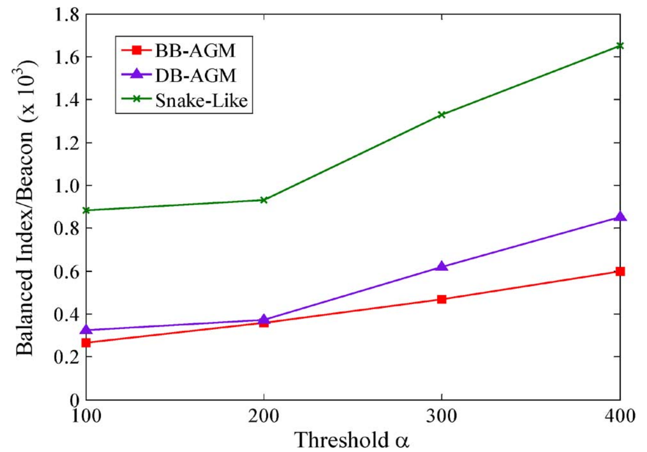

Fig. 20. Comparison of $BB-AGM$, $DB-AGM$, and *Snake-Like* in terms of BI by varying the value of α.

Fig. 20 shows the BI changed in each beacon by applying the $BB-AGM$ is smaller than the other mechanisms. Referring to Fig. 15, since the $DB-AGM$ consumes more energy than $BB-AGM$ when the anchor moves for balancing the location inaccuracies of the sensors, the $BB-AGM$ approach will significant improves the sizes of estimative regions and results in smaller routing error. Furthermore, a higher threshold value applied by the anchor can have better performance in terms of location inaccuracies of the sensors and routing error when the energy constraint of the mobile anchor is considered.

VII. Conclusions

To our knowledge, this is the first study that applies the mobile anchor to improve the location inaccuracy under the condition that all sensors are with different sizes of estimative regions. Firstly, the monitoring region is partitioned into grids and each grid is assigned with a weight value representing the localization benefit. Then the $BB-AGM$ and $DB-AGM$ approaches are proposed to select promising grids for broadcasting beacons so that the goals of minimizing and balancing the location inaccuracies of all sensors can be reached. Finally, a path construction algorithm is proposed to construct a path passing through the beacon locations and minimize the anchor's movement. Simulation results reveal that the proposed mechanism outperforms the *Snake-Like* and *Random* movements and hence obtains better results in terms of mean location error, localization efficiency and balance index.

References

[1] T. He, C. Huang, B. M. Blum, J. A. Stankovic, and T. Abdelzaher, "Range-free localization schemes for large scale sensor networks," in *Proc. ACM MobiCom*, Sep. 2003, pp. 81–95.

[2] C. Liu, K. Wu, and T. He, "Sensor localization with ring overlapping based on comparison of received signal strength indicator," in *Proc. IEEE MASS*, Oct. 2004, pp. 516–518.

[3] S. Zhang, J. Cao, L. Chen, and D. Chen, "Accurate and energy-efficient range-free localization for mobile sensor networks," *IEEE Trans. Mobile Computing*, vol. 9, no. 6, pp. 897–910, Jun. 2010.

[4] Y. Kwon and G. Agha, "Passive localization: Large size sensor network localization based on environmental events," in *Proc. ACM/IEEE IPSN*, Apr. 2008, pp. 3–14.
[5] M. Rudafshani and S. Datta, "Localization in wireless sensor networks," in *Proc. ACM/IEEE IPSN*, Apr. 2007, pp. 51–60.
[6] V. Vivekanandan and V. W. S. Wong, "Concentric anchor beacon localization algorithm for wireless sensor networks," *IEEE Trans. Vehicular Technol.*, vol. 56, no. 5, pp. 2733–2744, Sep. 2007.
[7] T. V. Srinath, "Localization in resource constrained sensor networks using a mobile beacon with in-ranging," in *Proc. IEEE WOCN*, Apr. 2006, pp. 301–305.
[8] J. P. Sheu, W. K. Hu, and J. C. Lin, "Distributed localization scheme for mobile sensor networks," *IEEE Trans. Mobile Computing*, vol. 9, no. 4, pp. 516–526, Apr. 2010.
[9] A. Galstyan, B. Krishnamachari, K. Lerman, and S. Pattem, "Distributed online localization in sensor networks using a moving target," in *Proc. ACM/IEEE Int. Symp. IPSN*, Apr. 2004, pp. 61–70.
[10] K. Kim and W. Lee, "MBAL: A mobile beacon-assisted localization scheme for wireless sensor networks," in *Proc. IEEE ICCCN*, Aug. 2007, pp. 57–62.
[11] G. Teng, K. Zheng, and W. Dong, "Adapting mobile beacon-assisted localization in wireless sensor networks," *Sensors*, vol. 9, no. 4, pp. 2760–2779, Apr. 2009.
[12] S. P. Kuo, H. J. Kuo, and Y. C. Tseng, "The beacon movement detection problem in wireless sensor networks for localization applications," *IEEE Trans. Mobile Computing*, vol. 8, no. 10, pp. 1326–1338, Oct. 2009.
[13] Z. Guo, Y. Guo, F. Hong, Z. Jin, Y. He, Y. Feng, and Y. Liu, "Perpendicular intersection: Locating wireless sensors with mobile beacon," *IEEE Trans. Vehic. Technol.*, vol. 59, no. 7, pp. 3501–3509, Sep. 2010.
[14] B. Xiao, H. Chen, and S. Zhou, "Distributed localization using a moving beacon in wireless sensor networks," *IEEE Trans. Parallel Distrib. Syst.*, vol. 19, no. 5, pp. 587–600, May 2008.
[15] B. Xiao, H. Chen, and S. Zhou, "A walking beacon-assisted localization in wireless sensor networks," in *Proc. IEEE ICC*, Jun. 2007, pp. 3070–3075.
[16] X. Zeng, R. Bagrodia, and M. Gerla, "GloMoSim: A library for parallel simulation of large-scale wireless networks," in *Proc. IEEE Workshop on Parallel Distributed Simul.*, May 1998, pp. 154–161.
[17] B. Karp and H. T. Kung, "GPSR: Greedy perimeter stateless routing for wireless networks," in *Proc. ACM MobiCom*, Aug. 2000, pp. 243–254.

Chao-Tsun Chang was born in Taipei, Taiwan. He received the Ph.D. degree in computer science and information engineering from National Central University, Taiwan, in 2006.

He has been with the faculty of the Department of Information Management, Hsiuping University of Science and Technology, Taiwan, as an Assistant Professor in 2006. In the recent 10 years, he has directed many researching projects including national NSC projects and information system developments. He is a member of the IEEE Computer Society and Communication Society. His current research interests include wireless sensor networks, Bluetooth radio networks, Ad Hoc wireless networks, and mobile computing.

Chih-Yung Chang (A'00) received the Ph.D. degree in Computer Science and Information Engineering from National Central University, Taiwan, in 1995.

He is currently a Full Professor with the Department of CSIE at Tamkang University, Taiwan.

Dr. Chang served as an Associate Guest Editor of many SCI indexed Journals, including *International Journal of Ad Hoc and Ubiquitous Computing* (IJAHUC 2011 & 2012), *International Journal of Distributed Sensor Networks* (IJDSN, 2012), *IET Communications* (2011), *Telecommunication Systems* (TS, 2010), *Journal of Information Science and Engineering* (JISE, 2008) and *Journal of Internet Technology* (JIT, 2004 & 2008). He was an Area Chair of *IEEE AINA*'2005, *TANET*'2000, *TANET*'2010, Vice Chair of *IEEE WisCom*'2005, *EUC*'2005 and *IEEE ITRE*'2005, *IEEE AINA* 2008, Program Co-Chair of *IEEE MNSA*'2005, *UbiLearn*'2006, *WASN*'2007, *ACM SAMnet*'2008, *IEEE AHUC*'2008, *iCube*'2010, *iCube*'2011, Workshop Co-Chair of *MSEAT*'2003, *MSEAT*'2004, *IEEE INA*'2005, *ICS*'2008, *NCS*'2009, *IEEE VCNA*'2009 and Publication Chair of *MSEAT*'2005 and *SCORM*'2006. Dr. Chang is a member of the IEEE Computer Society and Communication Society. His current research interests include Internet of Things, wireless sensor networks, Ad Hoc wireless networks, and WiMAX broadband technologies.

Chih-Yu Lin received the B.S. degree in computer science and information engineering from Aletheia University, Taiwan, in 2007, and the M.S. degree in Computer Science and Information Engineering from Tamkang University, Taiwan, in 2009, where he is currently working toward the Ph.D. degree in Department of Computer Science and Information Engineering.

His current research interests include Internet of Things, wireless sensor networks, Ad Hoc wireless networks, and WiMAX broadband technologies.

Mr. Lin received several scholarship grants in Taiwan and has participated in many wireless sensor network projects.